Title: Engineered bacteria launch and control an oncolytic virus

Authors: Zakary S. Singer[1,2]†, Jonathan Pabón[1]†, Hsinyen Huang[1], Charles M. Rice[2], Tal Danino[1,3,4]*

Affiliations:

[1]Department of Biomedical Engineering, Columbia University, New York, NY 10027, USA.

[2]Laboratory of Virology and Infectious Disease, The Rockefeller University, New York, NY 10065, USA.

[3]Herbert Irving Comprehensive Cancer Center, Columbia University, New York, NY 10032, USA.

[4]Data Science Institute, Columbia University, New York, NY 10027, USA.

* Corresponding author. Email: tal.danino@columbia.edu

† These authors contributed equally to this work

Abstract: The ability of bacteria and viruses to selectively replicate in tumors has led to synthetic engineering of new microbial therapies. Here we design a cooperative strategy whereby *S. typhimurium* bacteria transcribe and deliver the Senecavirus A RNA genome inside host cells, launching a potent oncolytic viral infection. Then, we engineer the virus to require a bacterially delivered protease in order to achieve virion maturation, demonstrating bacterial control over the virus. This work extends bacterially delivered therapeutics to viral genomes, and the governing of a viral population through engineered microbial interactions.

One-Sentence Summary: Bacteria are engineered to act as a synthetic "capsid" delivering Senecavirus A genome and controlling its spread.

Introduction

The broad range of applications that employ bacteria and viruses for therapy mirrors the diversity of the microbes themselves, as they target different tissues, microbiomes, and even intra- versus extra-cellular spaces. Examples of bacteria exploiting such characteristics include *E. coli* that detect irritable bowel disease (*1*), *S. epidermidis,* present in the skin microbiome, made to express tumor antigens (*2*), *M. pneumoniae* releasing an anti- *P. aeruginosa* bacteriocide (*3*), and *L. monocytogenes* and *Salmonella enterica* ser. *typhimurium* for tumor antigen and apoptotic protein delivery into host-cell cytoplasm (*4–6*).

Perhaps even more diverse are the viral families under investigation for therapy deployment. Examples of this assortment include the small ssDNA adeno-associated virus (AAV) whose natural and engineered serotypes provide tissue-specific targeting for monogenic gene therapies (*7*, *8*), the negative-stranded RNA Rabies Virus used for retrograde neuronal circuit tracing (*9*), the engineered mycobacteriophage to treat lethal, multi-drug resistant mycobacterial infections (*10*), and the diminutive but strongly cytopathic plus-stranded RNA viruses, like PVSRIPO, an engineered poliovirus derivative whose receptor binding capacity and host-translational determinants guide tropism for targeting glioblastoma (*11–15*). Together, microbes of broadly distinct evolutionary histories and cellular proclivities have each found utility in exploiting a specific application niche.

Considering the diverse range of benefits offered by various species, an innovative application of synthetic biology involves engineering multiple interacting entities, each with unique properties, to produce a consortium that achieves a collective objective. Applications that exploit this type of cooperation include cancer treatment, wound healing, and re-equilibration from gut dysbiosis (*16–22*). In each case, the division of labor between interacting species – even across kingdoms – presents an opportunity to exploit the advantages of the constituent elements.

Bacteria and viruses are generally considered separately in approaches to therapeutic delivery. However, in the case of natural infection, enteroviruses and enterobacteria directly bind to one another during co-infection, enhancing viral fitness (*23–25*). Here, we consider synthetic approaches for interspecies cooperation and apply the approach to a cancer model *in vivo*. Specifically, we engineer *S. typhimurium* to transcribe and deliver viral RNA inside cancer cells, launching a virus that spreads and directly lyses neighboring cells. We further engineer the virus to require a bacterially donated enzyme necessary for viral maturation and subsequent spread (**Fig. 1**). Such an approach where bacteria act as a dynamic envelope for a viral genome achieves a nested strategy for viral delivery, potentially provides shielding from innate or adaptive response; confers spatial specificity to the viral infection when made dependent on a bacterially delivered enzyme; and expands on pathogen associated molecular patterns (PAMPs) present as a result of multiple microbial penetrations. Together, this work demonstrates a complementation system for bacteria-mediated viral delivery and control.

Results

Engineered *S. typhimurium* autonomously launches viral RNA

To establish a bacterial platform capable of delivering viral RNAs, we use *S. typhimurium*, a naturally facultative intracellular bacterium. Upon uptake into the mammalian cell, these bacteria harboring genetically encoded environmental sensors will trigger *in situ* transcription of viral RNA, along with bacterial and vacuolar lysis proteins to enable delivery of the viral genome into the host cytoplasm. *S. typhimurium* achieves invasion into host cells via macropinocytosis, and then survives within the Salmonella Containing Vacuole (SCV) by expressing a battery of genes encoded on Salmonella Pathogenicity Islands 1 and 2 (SPI-1 and SPI-2), respectively (*26*). *S typhimurium* leveraging SPI-1 and 2 associated genes, promoters, secretion systems, and localization have been previously engineered for the delivery of proteins and plasmids (*5*, *27–34*). Here, we seek to exploit such a platform for delivering viral RNA capable of direct translation in the cytoplasm. As a result, this bypasses any need for nuclear

translocation of DNA-encoded therapeutics and subsequent expression before induction of apoptosis or pyroptosis by *Salmonella* (*35*, *36*). To achieve this requires developing a system that could efficiently deliver long nucleic acids, and could overcome the challenges associated with bacterially-delivered RNA such as sufficient RNA production, robust RNA integrity, RNA escape into the host cytoplasm, and the need for the host to survive through protein translation.

To spatially control the expression of the necessary synthetic elements of such a circuit, we looked to use genes whose activity is restricted to the intravacuolar space and chose SPI-2 promoters in order to drive viral RNA transcription *in situ* (**Fig 2A**). We evaluated SPI-2 promoters belonging to the *sseA* and *sseJ* genes, which are upregulated in the SCV (*29*, *30*, *37*, *38*). Using time-lapse imaging, we evaluated their temporal activity within individual cancer cells in the attenuated *S. typhimurium* strain LH1301 (Δ*aroA*, Δ*phoPQ*) (*39*) normalized to a constitutive GFP. We observed rapid activation of both promoters after entering mammalian cells, with no signal present during the initial 30-minute inoculation of bacteria, suggesting that these promoters are tightly regulated (**Fig 2B,C, S1A**).

Because prokaryotes do not incorporate 5'm7G caps (*40*), we chose to deliver viral RNAs that rely instead on cap-independent translation. Compatible with this requirement, Picornaviridae recruit ribosomes through an elaborate secondary structure at the 5' end of their genomes known as an internal ribosome entry site (IRES) (*41*). To evaluate how such a platform might function across a range of cell lines, we chose to utilize a poliovirus replicon, capable of replication in a number of different cell types (*42*) where its structural proteins are replaced with a fluorescent reporter, GFP. This further serves to uncouple viral genome replication from virion spread. By transfection, active replication of the viral genome leads to GFP levels 50x higher than when the encoded viral polymerase was mutationally inactivated, and in some cells, can reach three orders of magnitude above passively translated mRNA, highlighting the utility of using self-amplifying RNA (**Fig S1B**). To couple transcription of this viral RNA to intracellular sensing, the PsseA promoter drives the strongly processive T7-RNA polymerase, which in turn transcribes the viral RNA off a complementary cDNA genome encoded on a plasmid. When this circuit is transformed into *S. typhimurium* LH1301 and used to invade HeLa cells, these bacteria produce the full-length viral RNA, as measured by single-molecule fluorescence *in situ* hybridization (smFISH) using probes against the 3' end of the 5.5kb RNA (**Fig 2D**).

Once transcribed, the viral genome must exit the bacterium and translocate through the SCV into the cytoplasm of the mammalian host in order to replicate. To optimize efficiency of this 2-step translocation, we used two distinct bacterial lytic proteins: Lysis protein E from phage φX174 that disrupts bacterial membranes (*5*, *43–45*), allowing the viral RNA to exit the lysed bacterium, and Hemolysin E (HlyE), which forms pores in the SCV, allowing the viral RNA to enter the host cytosol (*46*). These genes are expressed under the control of intracellular sensing promoter PsseJ, and complemented by a deletion of the *sifA* gene in *S. typhimurium* LH1301, whose loss further disrupts SCV integrity (*6*, *47*). When *S. typhimurium* carries this circuit into HeLa cells, mCherry appears to diffuse out of the SCV, filling the cytoplasm of the host cell, while in the absence of these lytic proteins, mCherry remains punctate, indicating restricted localization within vacuoles (**Fig 2E**).

Finally, we couple viral transcription and the lysis circuit together in *S. typhimurium* and evaluate whether poliovirus replicon could be delivered into a range of cell types to launch replication. We observed strong GFP signals indicative of successful viral delivery and replication in both mouse and human cell lines including 4T1, B16, HCT116, HeLa, MC38, and H446 cells, albeit with differing efficiencies (**Fig 2F, S1C**). Furthermore, lysis via E and HlyE enabled dramatically more efficient delivery than in the absence of lytic proteins, or when *S. typhimurium* delivered plasmid-encoded GFP across most cell lines **(Fig S1D-E)**. Finally, to confirm that this was not simply passive translation of the incoming genomic viral RNA, we stained cells with an antibody against long double-stranded RNA (dsRNA), a product of active viral replication, and observed strong signals in cells that were also GFP positive (**Fig**

2G). Together, these data show that lysing *S. typhimurium* is capable of successfully delivering actively replicating viral RNA.

Delivery of full-length oncolytic virus by engineered *S. typhimurium* clears subcutaneous SCLC tumors

We next tested the ability of this system to deliver a therapeutically relevant full-length oncolytic virus, Senecavirus A (SVA), known to infect H446 small cell lung cancer cells and other cells with neuroendocrine origins. (*48–51*). Because cells infected with *S. typhimurium* frequently die via induction of apoptosis and pyroptosis (*35*), a spreading virus could infect surrounding *S. typhimurium*-free cells, augmenting the overall therapeutic effect (**Fig 3A**).

For such a system to function, bacteria and virus must both be able to infect the target population, with the former not directly inhibiting the latter. Using SVA with a genome encoded GFP (SVA-GFP) (*52*), we measured whether and how viral spread was affected when introduced one hour after bacterial pre-infection in H446 cells, a small cell lung cancer (SCLC) line. At 24 HPI there was no measurable reduction in the spread of virus in the presence or absence of bacteria (**Fig S2A**).

In lysing *S. typhimurium*, we replaced the poliovirus replicon with SVA-GFP and inoculated H446s to look for successful initial delivery events from bacteria and a subsequent capacity for spread throughout the same culture. The first wave of SVA-infected cells was observed at approximately 8 hours following bacteria inoculation, with viral spreading occurring continuously throughout the subsequent 60 hours (**Fig 3B, Supplementary Movie 1**).

To determine whether similar viral launch and spread could translate into an *in vivo* setting, we first xenografted nude mice with bilateral hind flank H446 tumors. Then, only their right tumors were injected intratumorally (IT) with lysing *S. typhimurium* carrying SVA-NanoLuc (a luminescent reporter) and imaged over time for luminescence. Two days post-infection, some right-flank tumors showed luminescence so strong that it saturated the detector (**Fig 3C**). Furthermore, at day four, the signal was additionally observable in left tumors that had not been injected with bacteria, suggesting productive viral infection in the right tumors and sufficient titer capable of viral translocation to left-flank tumors. In contrast, control bacteria recombinantly expressing their own luminescent protein, luxCDABE, under the control of PsseA, showed no detectable translocation to left tumors over the same time (**Fig S2B-C**). Tumor volume measurements over more than 40 days showed complete regression of both left and right tumors in the treatment group within two weeks, whereas all tumors treated with only buffer or lysing bacteria alone continued to grow until reaching maximum allowable sizes (**Fig 3D, S2D**). Mice experienced no decline in weight, and negligible bacteria in the liver or spleen, despite appreciable loads present in the tumors, suggesting no adverse response to bacterial injections (**Fig S2E, F**). Taken together, lysing *S. typhimurium* is capable of launching a viral infection and clearing H446 tumors *in vivo*.

Engineered synergy between virus and bacteria controls viral polyprotein cleavage and resulting spread

Improving efficacy and safety profiles of oncolytic viruses is achieved either at the cell-surface level, where the receptor-binding domain is altered to recognize a target cell more specifically, or intracellularly, where replication of the virus is modulated positively or negatively by cell-type specific cytoplasmic or nuclear determinants (*53*). Having constructed a bacterial platform that successfully delivers both viral RNA as well as proteins into the host cytoplasm, we considered how further cooperation between these microbes could present a novel strategy for selectively regulating viral life cycles.

In the life cycle of picornaviruses, all proteins are translated first as one large open reading frame. This polyprotein must be then cleaved into individual constituents entirely by virally encoded proteases (*54*). Thus, shifting a cleavage event to an orthogonal protease expressed by bacteria would enable a control over the viral life cycle and such a protease might be delivered simultaneously by lysing bacteria

(**Fig 4A**). Due to its potential for recombinant expression and thorough characterization, we chose Tobacco Etch Virus protease (TEVp) as the orthogonal protease (*55*). Furthermore, TEVp has the flexibility to recognize nearly all residues at the final position of the cognate TEV cleavage site (TEVs) sequence (ENLYFQ^G) where cleavage occurs between the last two amino acids (*55*). This allows for the ability to retain the native N-terminal residue of the downstream protein following successful cleavage.

Investigating which natural cleavage site in SVA might be amenable to TEVs substitution, we preferentially screened all four sites flanking each structural protein, abrogating the natural cleavage sequence in the process. This would enable successful packaging of the virus in cells containing the protease, followed by viral entry and replication in surrounding cells. However, should the surrounding cell not contain TEVp, further spread would be restricted. We engineered each of these four potential variants and transfected them either into wild-type H446 cells, or H446s constitutively expressing TEVp, and looked for conditional spreading (**Fig 4B**). When the TEVs was placed between the nonstructural Leader protein and the first structural protein VP4, the spreading of this variant became entirely dependent on TEVp and was capable of infecting surrounding cells at a rate equivalent to wild-type virus (**Fig 4C-D**).

In order to couple the spread of this variant to co-infecting bacteria, we engineered lysing *S. typhimurium* to express TEVp under the control of a second PsseA intracellularly sensing promoter. Additionally, we incorporated a series of mutations to TEVp previously shown to improve the solubility of the protease (*56*, *57*) (**Fig S3A**). When the bacteria delivered a TEVp-dependent virus without bacterially produced TEVp, the virus launches but then fails to spread, as expected (**Fig 4E, left**). However, when the *S. typhimurium* simultaneously delivered both the TEVp-dependent virus as well as TEVp, localized foci of spreading infection appeared (**Fig 4E, right**).

We next proceeded to evaluate this platform *in vivo,* first aiming to characterize the stability of the engineered genome, owing to the high error rate of RNA-dependent RNA polymerases (RdRps) and potential to mutate away from TEVp-dependence (*58*). Tumors were injected IT with *S. typhimurium* delivering wild-type SVA-NanoLuc and compared to TEVs-SVA-NanoLuc with co-delivered protease. Over the course of one week, the luminescence of the group receiving bacterially delivered wild-type SVA-NanoLuc continued to increase rapidly. In contrast, the signal from tumors injected with bacterially delivered TEV-dependent SVA remained lower than wild-type through day eight, but then began to increase (**Fig S3B, top**). Sequencing viral RNA extracted from tumors that received the TEVs-SVA revealed that three out of five had a single-nucleotide polymorphism (SNP) in the TEVs, yielding two different ways of producing an identical phenylalanine-to-leucine (F->L) substitution (**Fig S3B, bottom**). When this mutation was cloned into the viral genome and transfected directly into H446 with or without TEVp, we observed that this mutation was sufficient to achieve TEVp-independent spreading (**Fig S3C**); a leucine at this site recapitulates the residue normally at this position immediately upstream of the scissile Q^G cleavage site in the wild-type virus.

To prevent this escape mutation from occurring, an optimal TEVs sequence would be one where the codon for phenylalanine requires more than one SNP to revert into a leucine. While no codon like this for phenylalanine exists, previous interrogation of TEVs revealed that a cysteine at the phenylalanine site maintained TEVp-mediated cleavage, while being two SNPs away from reverting to a leucine (*59*). Indeed, an SVA variant with the modified TEVs sequence of ENLY**C**Q^G only spread in the presence of TEVp, though at slightly reduced efficiency compared to the WT TEVs (**Fig 4F, S3C**). Thus, we were able to construct a mutationally resistant variant of TEVp-dependent SVA (denoted rTEVs-SVA).

Carrying this new variant, groups of mice received lysing *S. typhimurium* with and without TEVp, or WT-SVA alone. 24 hours following injection, tumors were harvested, homogenized, and assayed for luminescence *ex vivo* as a readout for replication originating from bacterial launch, as well as for viral titer measurements as an indication of successful packaging of the virus. The initial luminescence as measured *ex vivo* was statistically indistinguishable between groups, showing equivalent initial delivery

from bacteria of WT virus compared to TEVp-dependent virus (**Fig S3D**). Similarly, the number of viral particles produced by cells infected with TEVp-dependent virus was also statistically the same as WT virus delivery at launch (**Fig 4G**). In contrast, no infectious particles were recovered when TEVp-dependent virus was delivered in the absence of TEVp, as expected (**Fig 4G**). Furthermore, when naive cells *in vitro* were infected with tumor-harvested WT virus, spreading was observed, while tumors containing TEVp-dependent virus showed initial replication, but no further spread (**Fig S3E**). Together, these data suggest that the initial launch and production of infectious viral particles are equally efficient between both WT and TEV-dependent viruses, and that engineered virus launched from bacteria was indeed TEVp-dependent.

Finally, when a cohort of mice injected with lysing *S. typhimurium* delivering TEVp-dependent virus with and without protease was measured longitudinally, we observed that luminescence from this mutation-resistant variant continued to remain present for up to two weeks following a single injection, while virus delivered without protease showed a complete loss of signal over the same time period. Over this time course, no increasing luminescent signals were observed, suggesting that reversion to TEVp-independence did not occur (**Fig 4H, S3F**).

Discussion

This work explored synthetic strategies to design multiple levels of synergy between two clinically relevant microbes - *S. typhimurium* and Senecavirus A. By utilizing bacteria as a dynamic and engineerable "viral capsid", we delivered replicons and full-length viral RNAs into the host cytoplasm, with SVA entirely clearing subcutaneous SCLC tumors. Furthermore, the bacterial launch of replicons in a range of mouse and human cell lines demonstrates the ability to deliver non-spreading viral RNAs while bypassing the receptor-mediated limitations of the native viral capsid proteins. Noting that the bacterial vehicle is able to simultaneously deliver proteins and nucleic acids, we devised a strategy to build further synergy: a modified virus whose protein maturation depends on a bacterially provided protease (TEVp), by substituting a natural cleavage site in the virus with an orthogonal one (TEVs). Together, we developed a multi-layered engineering approach for coordinating a two-microbe system for oncolytic application.

Delivery of nucleic acids by bacteria, or bactofection, has been previously applied, for example by *Agrobacterium* for CRISPR/CAS9 gene-editing in wheat (*60*); *L. monocytogenes*, *E. coli* and *S. typhimurium* for siRNAs, short ORF-containing RNAs for GFP, and plasmids (*28*, *36*, *61–69*), albeit with efficiencies that would hinder viral RNA delivery. Leveraging the flexible tools available for genetic engineering in *S. typhimurium*, we were able to deliver large viral RNAs more efficiently across a broad range of cell types than those previously reported via engineered *S. typhimurium* strains (*64*). Further, these vectors allow for subsequent productive viral infections. Building on previous work for intracellular delivery, here the active replication of viral RNA causes a cytopathic effect in its initial host cell, while also enabling spread to surrounding cells potentially uninfected by bacteria, thereby enhancing therapeutic effect. However, while SVA does not natively infect murine cells, the athymic model used here permits study in a relevant human cell line and provides the framework for implementing a consortium of cooperative engineered microbes *in vivo*.

Our efforts to insert an orthogonal cleavage site into the virus highlight the importance of addressing the mutability of RNA viruses. RNA-dependent RNA polymerases incorporate an incorrect base at a rate of roughly 1 in 10,000 (*70–73*). Here, we attempted to mitigate mutational escape by first identifying the most common escape mechanism *in vivo*, a reversion to leucine at the P2 position of the TEVs, by swapping the TEVs' P2 amino acid to one that cannot revert to a leucine without requiring two simultaneous SNPs. Therefore, the likelihood of reversion by two independent mutations simultaneously occurring in the cleavage site geometrically reduces the escape probability. However, alternate types of mutations, such as wholesale deletions of our orthogonal sequence may also occur, though were not

observed here. Insertion of additional TEVs', or even additional protease/cleavage site pairs, could further increase the robustness of this system and even enable construction of logic-gated viral replication and spread.

Through the use of simultaneous protein and RNA delivery, genetic circuits composed of proteins, nucleic acids, and a microbial consortium all combine to produce a synergistic and unique output with therapeutic applications.

Figures

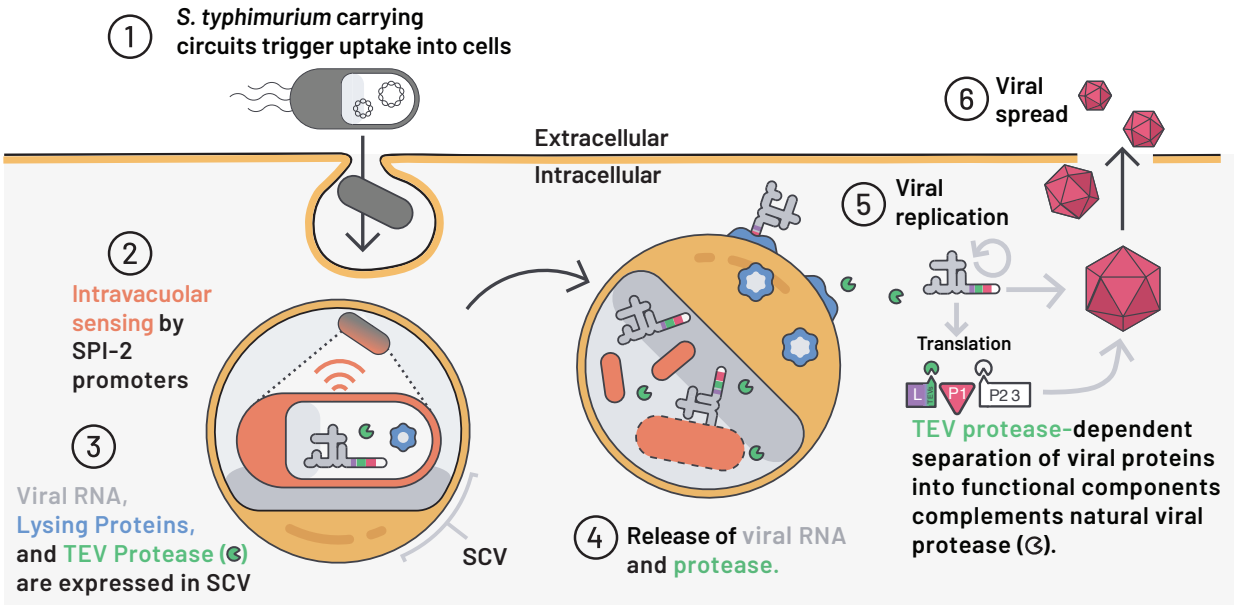

Figure 1: Programmed *S. typhimurium* autonomously lyse in host cytoplasm to launch viral RNA and an essential orthogonal viral protease. (1) *S. typhimurium* carrying synthetic circuits enter mammalian cells via natural effectors encoded on Salmonella Pathogenicity Island 1 (SPI-1). **(2)** Internalized *S. typhimurium* within a Salmonella Containing Vacuole (SCV) is designed to sense the intravacuolar space, triggering activation of SPI-2 promoters. **(3)** Engineered SPI-2 promoters are used to drive the production of viral RNAs (Poliovirus replicon, Senecavirus A (SVA), and TEV protease-dependent SVA), lysing proteins hemolysin-E (HlyE) and E from phage φX174, and TEV protease. **(4)** Upon successful bacterial and vacuolar lysis, viral RNAs and TEV protease are released into the host cytoplasm. **(5)** Viral RNAs are translated in the cytoplasm and viral replication is initiated. The maturation of viral particles derived from TEV-dependent SVA requires cleavage by both a virally encoded protease and a bacterially donated TEV protease. The latter cuts at the cognate TEV sequence engineered between the Leader (L) protein and the first protein (VP4) of the structural genes (P1), enabling viral RNA encapsidation. **(6)** Infectious particles are released into the extracellular space to infect neighboring cells.

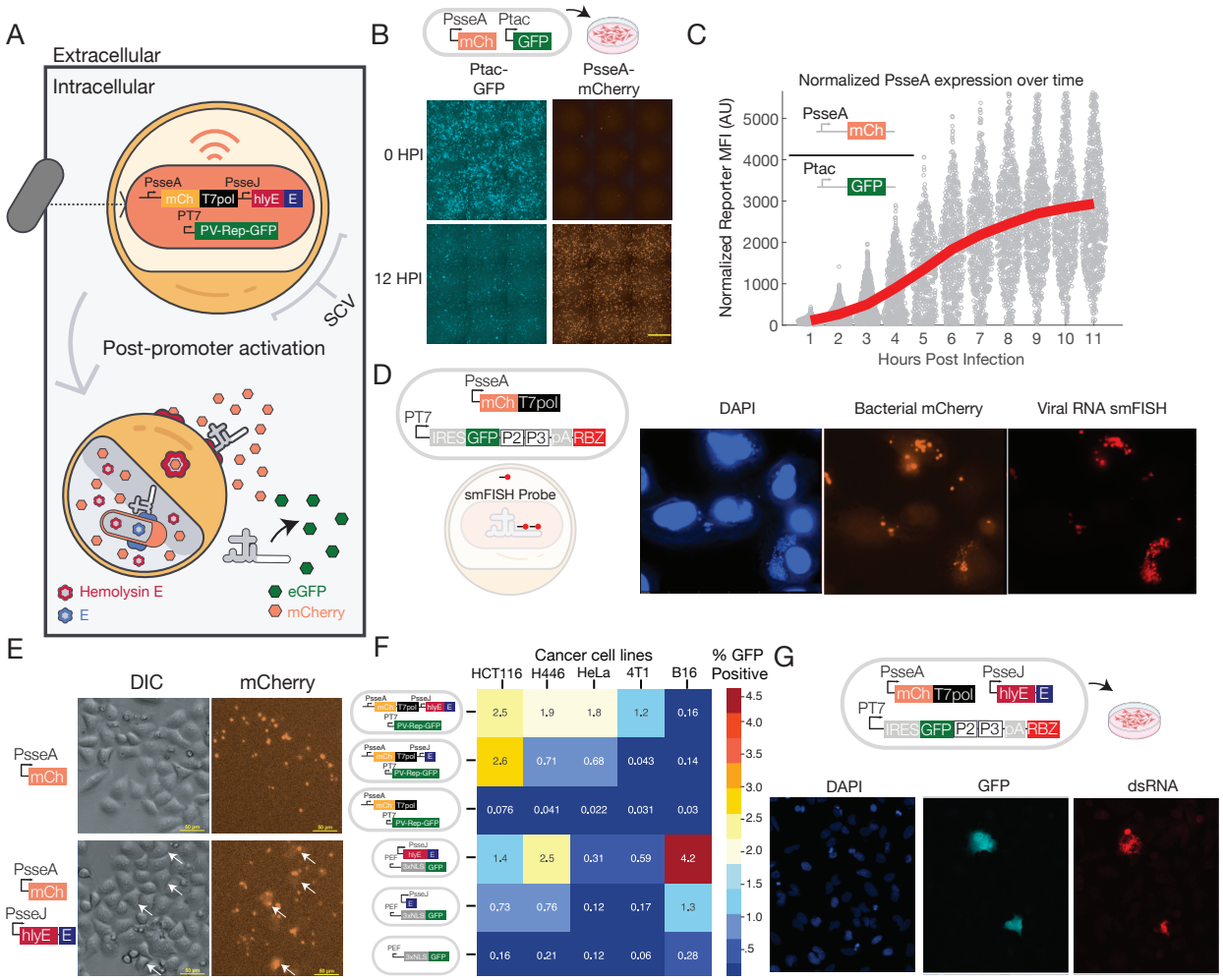

Figure 2: Engineered bacteria deliver self-replicating RNA into the cytoplasm of host cells. (A) Intracellular *S. typhimurium* activates SPI-2 promoters PsseA and PsseJ, to drive mCherry expressed by either promoter. After internalization of bacterium and PsseA-mCherry+T7pol/PsseJ-HlyE+E activation**,** intravacuolar *S. typhimurium* lyse the SCV and themselves, releasing mCherry and T7-driven poliovirus-replicon RNA into the cytoplasm where replication and translation produce reporter GFP. **(B)** Microscopy images of HeLa cells inoculated with *S. typhimurium* at multiplicity of infection (MOI) 50 carrying Ptac-GFP and PsseA-mCherry plasmids. The top panels show constitutive Ptac-GFP and SCV-induced PsseA-mCherry signals at 0 HPI. The bottom panels show respective signals 12 HPI. Scale = 500µm. **(C)** Quantification of PsseA activation is shown as the mean fluorescent intensities (MFI) of mCherry divided by GFP, where each dot represents a single HeLa cell. At each time point the average over all cells is plotted as a red point on the red line. The initial value is taken 1 hour post-infection (HPI). **(D)** (Left), Top- circuit diagram of proteins produced by PsseA activation and PT7-driven poliovirus replicon. Bottom- Schematic of smFISH probes binding specifically to the 3' end of the viral RNA transcribed by bacteria. (Right) Micrograph showing DAPI staining of both mammalian and bacterial DNA (blue), PsseA-mCherry fluorescence from *S. typhimurium* inside SCVs (orange) and fluorescent signal from probes specific to viral RNA produced (red). **(E)** Top panels show representative DIC and mCherry signals of HeLa cells inoculated with *S. typhimurium* at an MOI 50 carrying a PsseA-mCherry plasmid. Bottom panels are HeLa cells inoculated with *S.*

typhimurium at MOI 50 carrying the mCherry reporter and lysing proteins. The white arrow indicates a cell with an mCherry signal diffusing through the host cytoplasm. Scale bar is 50µm. **(F)** The efficiency of replicon delivery (GFP expressed off poliovirus replicon) in HCT116, H446, HeLa, 4T1, B16 cells and plasmid delivery (GFP expressed off plasmid with pEF-promoter and repeating nuclear localization signals) using *S. typhimurium* strains that either lyse with HlyE and E proteins, the E protein alone or do not lyse. **(G)** Bacteria with lysing circuit and virus-encoding plasmid are used to inoculate HeLa cells. DAPI indicates nuclear staining; GFP fluorescence is derived from viral RNA reporter. Red fluorescence signal is an anti-647 secondary antibody against an anti-dsRNA antibody indicating active replication of viral RNA.

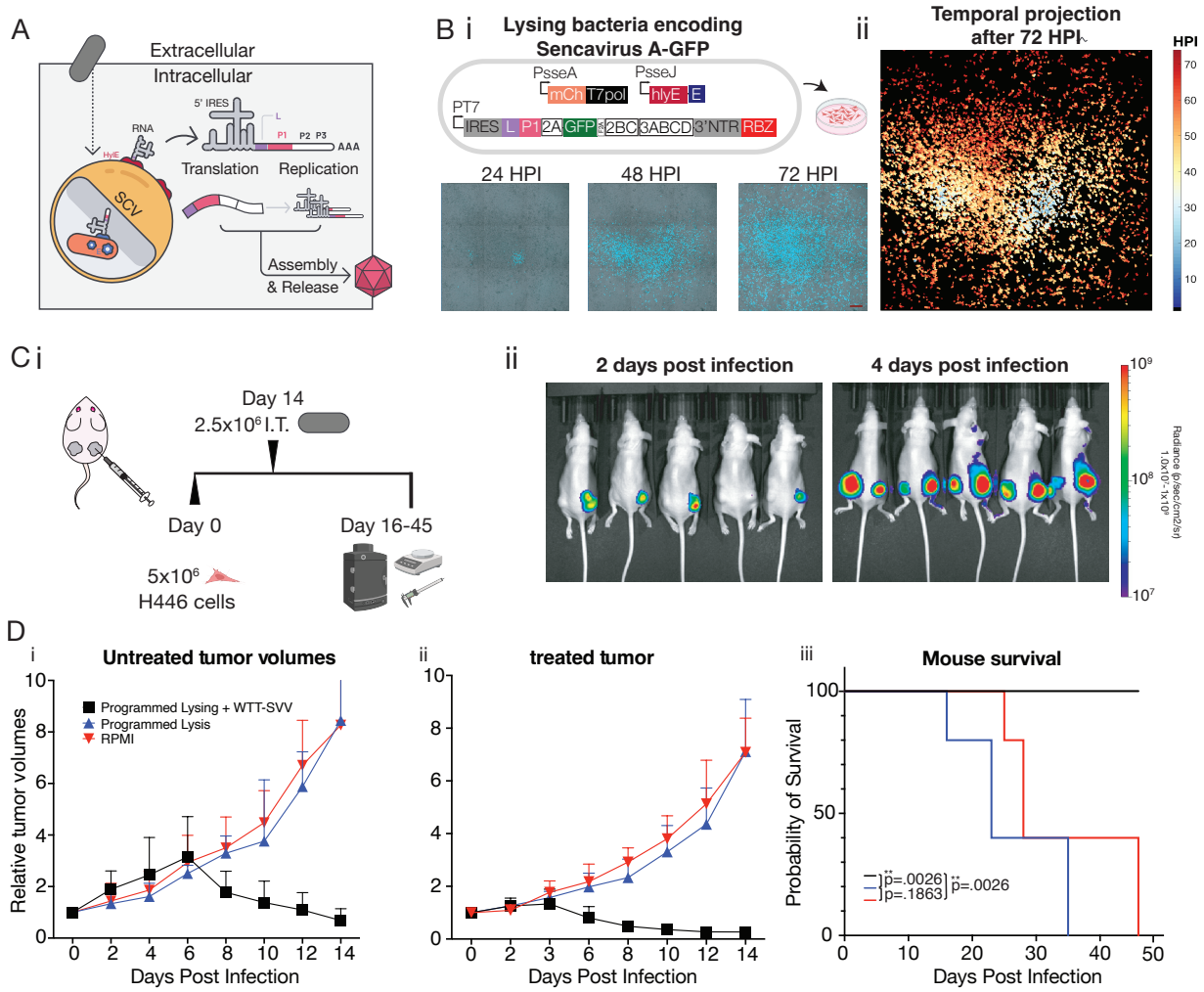

Figure 3: Lysing *S. typhimurium* launch full-length oncolytic virus Senecavirus A (SVA) and clears subcutaneous tumors. (A) Schematic of *S. typhimurium* SPI-2 driven production of viral RNA and lysing proteins allowing the escape of viral RNA from the *Salmonella* containing vacuole (SCV) and *S. typhimurium*. Upon release of RNA into the cytoplasm, IRES-mediated translation produces viral proteins necessary for replication of RNA, assembly of the capsid, and packaging of the viral genome into its capsid. **(B)** H446 cells inoculated with (i, top) MOI 25 *S. typhimurium* Δ*sifA* carrying SPI2-driven lysis and reporter plasmid, along with SVA-GFP plasmid. (i, bottom) Time-lapse microscopy at three-time points of spreading SVA-GFP as launched from bacteria. Scale bar = 500µm. (ii) Time course of SVA-GFP infection throughout the course of the 72-hour acquisition period, projecting time as a color with initial events represented in light blue hues and later events passing through yellow and red hues. **(C)** (i) Experimental outline of *in vivo* experiment where nude mice were engrafted with H446 cells on bilateral flanks, and right flanks were intratumorally injected with $2.5x10^6$ lysing *S. typhimurium* carrying SVA-Nanoluc RNA when tumors reached approximately 150 mm^3 14 days later. (ii) IVIS images of nude mice injected with NanoLuc substrate intratumorally 2 days and 4 days post bacterial inoculation. **(D)** (i) Growth kinetics of left tumors treated with lysing *S. typhimurium* with WT-SVA (black), lysing *S. typhimurium* only (blue), and RPMI (red) over the first two weeks post-inoculation. The mean and standard deviation of the mean are plotted on the graph. (ii) Growth kinetics of right tumors. (iii) Survival curves for mice treated with groups annotated in D (i). Survival benefit observed by log-rank test for each survival curve.

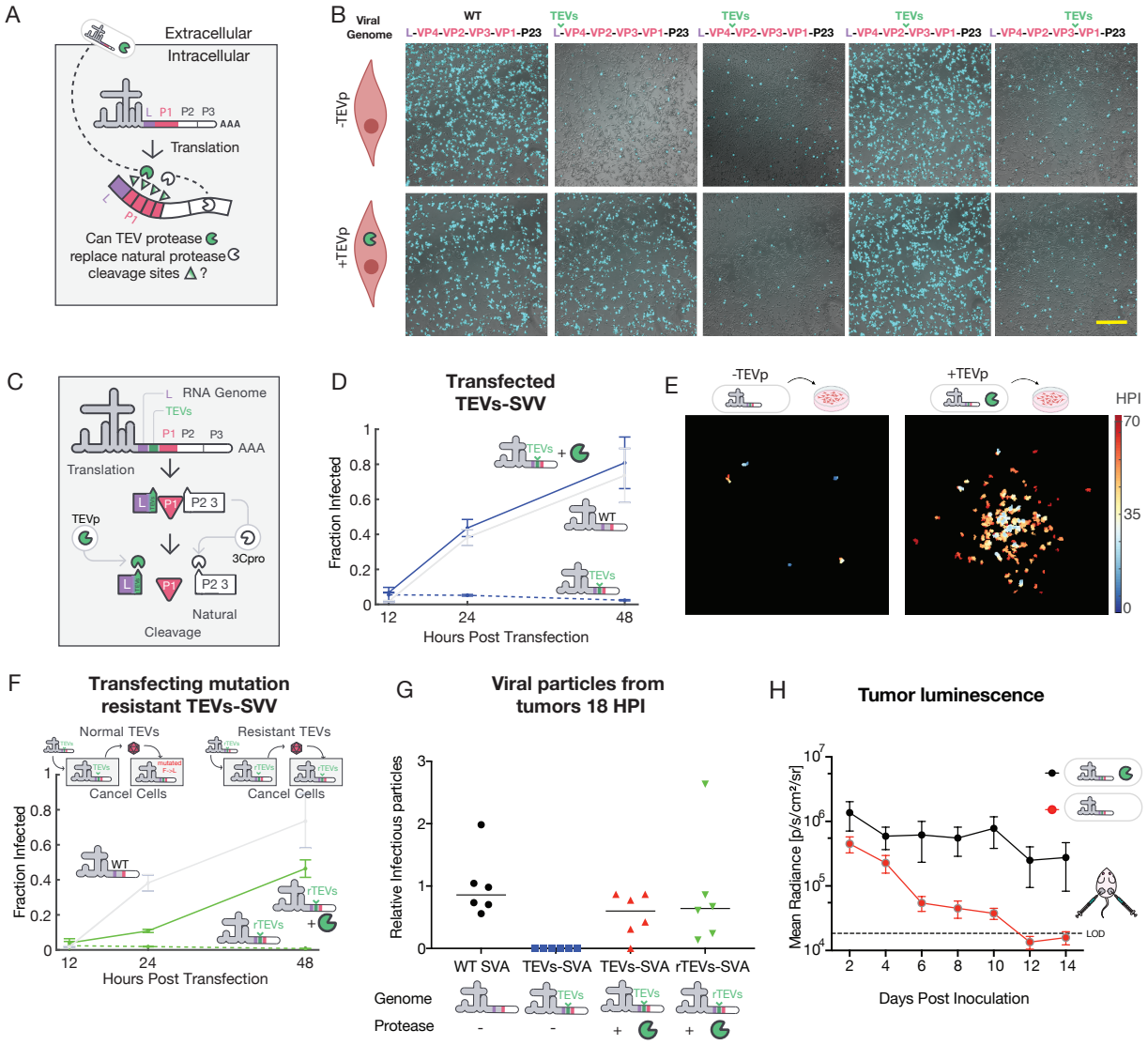

Figure 4: Engineering control over natural viral protein separation enables dependence on bacterially delivered protease. (A) Schematic of viral protease cleavage at natural cleavage sites (white arrow shade) in between the L-protein and individual structural viral proteins, and their reprogramming as possible sites for exogenous protease cleavage (green arrow shade). **(B)** H446 cells transfected with piggybac plasmids to express integrated TEV protease (bottom row) and non-transfected H446 cells (top row) were subsequently transfected with 500 ng of WT-SVA and SVA RNA engineered to express TEV cleavage sequence motifs in place of native cleavage between structural proteins. Images taken 24 hours post-transfection at 10x. Scale bar is 500µm. **(C)** Illustration of TEV-mediated cleavage between L-protein and VP4 in the P1 structural protein domain. TEV site is cleaved by *S. typhimurium*-provided TEV protease, leaving a 6 amino acid C-terminal addition (ENLYFQ) on L protein, while all other cleavage sites are naturally cleaved by the SVA-proteases. **(D)** Fraction of H446 cells expressing WT-SVA-GFP (grey), TEVs-SVA-GFP (blue dotted), and TEVs-SVA-GFP + TEVp (solid blue) post-transfection at 12, 24, and 48 hrs. **(E)** H446 cells inoculated with *S. typhimurium* carrying TEVs-SVA-GFP with (right) and without (left) TEVp at MOI 50. Time course of bacterially delivered virus with (right) and without (lef)

protease; images shown are a projection of time as a color with initial events represented in light blue hues and later events passing through yellow and red hues over the course of the 72h experiment **(F)** Representation of TEV site mutation (ENLYFQ^G→ENLYLQ^G) addressed by converting TEVs to a mutationally resistant (rTEVs) site (ENLYCQG) above plot for fraction of H446 cells expressing WT-SVA-GFP (grey), rTEVs-SVA-GFP (green dotted), and rTEVs-SVA-GFP + TEVp (solid green) post-transfection at 12, 24, and 48 hrs. **(G)** Tumors treated with lysing *S. typhimurium* carrying WT-SVA-NanoLuc without TEV protease, TEVs-SVA-NanoLuc with and without TEV protease, and rTEVs-SVA-NanoLuc with TEV protease were excised 18 HPI. Naive H446 cells were inoculated with viral particles from tumor solutions freeze-thawed and centrifuged for viral particle isolation. Each point within a bar represents naive H446 cells infected with viral particles divided by the average of virally infected naive H446 cells from the WT-SVA group. ANOVA evaluation determined no significant difference in means in the WT-SVA-NanoLuc without TEVp, TEVs-SVA-NanoLuc with TEV protease, and rTEVs-SVA-NanoLuc with TEV protease groups. No indication of infectious viral particle production from Naive H446 cells inoculated with tumors treated with *S. typhimurium* carrying TEVs-SVA-NanoLuc without TEV protease, ANOVA test between all groups except TEVs-SVA-without-protease indicated p=0.46. **(H)** *In vivo* luminescent signals from nude mice with bilateral hind flank tumors inoculated with *S. typhimurium* expressing rTEVs-SVA-NanoLuc with (black) and without (red) TEV protease. Each point on the graph illustrates the mean and standard deviation of the luminescent signal of n=10 tumors at each time point.

Acknowledgments:

SVV-001-GFP was a kind gift of Professor JT Poirier at NYU Langone.

Funding:

Department of Defense grant BC160541 (TD)

National Institutes of Health grant NIH R01EB029750 (TD)

National Institutes of Health grant NRSA F32CA225145 (ZSS)

Author contributions:

Project Administration: CMR, TD

Supervision: ZSS, TD

Conceptualization: ZSS, TD

Methodology: JP, ZSS, TD

Investigation: JP, ZSS, TD

Visualization: JP, ZSS, TD

Funding acquisition: ZSS, TD

Software: JP, ZSS

Writing – original draft: JP, ZSS, TD

Writing – review & editing: JP, ZSS, TD

Competing interests: ZSS, JP, and TD have filed a provisional patent application with the US Patent and Trademark Office related to this work.

Data and materials availability: All data, materials, and code are available upon request form the corresponding author.

Supplementary Materials

Materials and Methods

Figs. S1 to S3

References

1. J. Y. Xia, C. Hepler, P. Tran, N. J. Waldeck, J. Bass, A. Prindle, Engineered calprotectin-sensing probiotics for IBD surveillance in humans. *Proc Natl Acad Sci U S A*. **120**, e2221121120 (2023).
2. Y. E. Chen, D. Bousbaine, A. Veinbachs, K. Atabakhsh, A. Dimas, V. K. Yu, A. Zhao, N. J. Enright, K. Nagashima, Y. Belkaid, M. A. Fischbach, Engineered skin bacteria induce antitumor T cell responses against melanoma. *Science*. **380**, 203–210 (2023).
3. R. Mazzolini, I. Rodríguez-Arce, L. Fernández-Barat, C. Piñero-Lambea, V. Garrido, A. Rebollada-Merino, A. Motos, A. Torres, M. J. Grilló, L. Serrano, M. Lluch-Senar, Engineered live bacteria suppress Pseudomonas aeruginosa infection in mouse lung and dissolve endotracheal-tube biofilms. *Nat Biotechnol*. **41**, 1089–1098 (2023).
4. Y. Chen, D. Yang, S. Li, Y. Gao, R. Jiang, L. Deng, F. R. Frankel, B. Sun, Development of a Listeria monocytogenes-based vaccine against hepatocellular carcinoma. *Oncogene*. **31**, 2140–2152 (2012).
5. V. Raman, N. Van Dessel, C. L. Hall, V. E. Wetherby, S. A. Whitney, E. L. Kolewe, S. M. K. Bloom, A. Sharma, J. A. Hardy, M. Bollen, A. Van Eynde, N. S. Forbes, Intracellular delivery of protein drugs with an autonomously lysing bacterial system reduces tumor growth and metastases. *Nat Commun*. **12**, 6116 (2021).
6. E. M. Camacho, B. Mesa-Pereira, C. Medina, A. Flores, E. Santero, Engineering Salmonella as intracellular factory for effective killing of tumour cells. *Sci Rep*. **6**, 30591 (2016).
7. J. R. Mendell, S. Al-Zaidy, R. Shell, W. D. Arnold, L. R. Rodino-Klapac, T. W. Prior, L. Lowes, L. Alfano, K. Berry, K. Church, J. T. Kissel, S. Nagendran, J. L'Italien, D. M. Sproule, C. Wells, J. A. Cardenas, M. D. Heitzer, A. Kaspar, S. Corcoran, L. Braun, S. Likhite, C. Miranda, K. Meyer, K. D. Foust, A. H. M. Burghes, B. K. Kaspar, Single-Dose Gene-Replacement Therapy for Spinal Muscular Atrophy. *New England Journal of Medicine*. **377**, 1713–1722 (2017).
8. S. Russell, J. Bennett, J. A. Wellman, D. C. Chung, Z.-F. Yu, A. Tillman, J. Wittes, J. Pappas, O. Elci, S. McCague, D. Cross, K. A. Marshall, J. Walshire, T. L. Kehoe, H. Reichert, M. Davis, L. Raffini, L. A. George, F. P. Hudson, L. Dingfield, X. Zhu, J. A. Haller, E. H. Sohn, V. B. Mahajan, W. Pfeifer, M. Weckmann, C. Johnson, D. Gewaily, A. Drack, E. Stone, K. Wachtel, F. Simonelli, B. P. Leroy, J. F. Wright, K. A. High, A. M. Maguire, Efficacy and safety of voretigene neparvovec (AAV2-hRPE65v2) in patients with RPE65-mediated inherited retinal dystrophy: a randomised, controlled, open-label, phase 3 trial. *Lancet*. **390**, 849–860 (2017).
9. I. R. Wickersham, S. Finke, K.-K. Conzelmann, E. M. Callaway, Retrograde neuronal tracing with a deletion-mutant rabies virus. *Nat Methods*. **4**, 47–49 (2007).
10. R. M. Dedrick, C. A. Guerrero-Bustamante, R. A. Garlena, D. A. Russell, K. Ford, K. Harris, K. C. Gilmour, J. Soothill, D. Jacobs-Sera, R. T. Schooley, G. F. Hatfull, H. Spencer, Engineered bacteriophages for treatment of a patient with a disseminated drug-resistant Mycobacterium abscessus. *Nat Med*. **25**, 730–733 (2019).
11. R. M. Conry, B. Westbrook, S. McKee, T. G. Norwood, Talimogene laherparepvec: First in class oncolytic virotherapy. *Hum Vaccin Immunother*. **14**, 839–846 (2018).
12. A. Desjardins, M. Gromeier, J. E. Herndon, N. Beaubier, D. P. Bolognesi, A. H. Friedman, H. S. Friedman, F. McSherry, A. M. Muscat, S. Nair, K. B. Peters, D. Randazzo, J. H. Sampson, G. Vlahovic, W. T. Harrison, R. E. McLendon, D. Ashley, D. D. Bigner, Recurrent Glioblastoma Treated with Recombinant Poliovirus. *N Engl J Med*. **379**, 150–161 (2018).
13. S. J. Russell, K.-W. Peng, J. C. Bell, Oncolytic virotherapy. *Nat Biotechnol*. **30**, 658–670 (2012).
14. C. Goetz, E. Dobrikova, M. Shveygert, M. Dobrikov, M. Gromeier, Oncolytic poliovirus against malignant glioma. *Future Virol*. **6**, 1045–1058 (2011).
15. H. L. Kaufman, F. J. Kohlhapp, A. Zloza, Oncolytic viruses: a new class of immunotherapy drugs. *Nat Rev Drug Discov*. **14**, 642–662 (2015).

16. M. Perez, A. Ntemiri, H. Tan, H. M. B. Harris, H. M. Roager, C. Ribière, P. W. O'Toole, A synthetic consortium of 100 gut commensals modulates the composition and function in a colon model of the microbiome of elderly subjects. *Gut Microbes*. **13**, 1–19 (2021).
17. R. El Hage, E. Hernandez-Sanabria, M. Calatayud Arroyo, R. Props, T. Van de Wiele, Propionate-Producing Consortium Restores Antibiotic-Induced Dysbiosis in a Dynamic in vitro Model of the Human Intestinal Microbial Ecosystem. *Front Microbiol*. **10**, 1206 (2019).
18. L. Li, C. Yang, B. Ma, S. Lu, J. Liu, Y. Pan, X. Wang, Y. Zhang, H. Wang, T. Sun, D. Liu, Hydrogel-Encapsulated Engineered Microbial Consortium as a Photoautotrophic "Living Material" for Promoting Skin Wound Healing. *ACS Appl Mater Interfaces*. **15**, 6536–6547 (2023).
19. A. Aalipour, F. Le Boeuf, M. Tang, S. Murty, F. Simonetta, A. X. Lozano, T. M. Shaffer, J. C. Bell, S. S. Gambhir, Viral Delivery of CAR Targets to Solid Tumors Enables Effective Cell Therapy. *Mol Ther Oncolytics*. **17**, 232–240 (2020).
20. R. L. Vincent, C. R. Gurbatri, A. Redenti, C. Coker, N. Arpaia…, Probiotic-guided CAR-T cells for universal solid tumor targeting. *bioRxiv* (2021).
21. T. Tanoue, S. Morita, D. R. Plichta, A. N. Skelly, W. Suda, Y. Sugiura, S. Narushima, H. Vlamakis, I. Motoo, K. Sugita, A. Shiota, K. Takeshita, K. Yasuma-Mitobe, D. Riethmacher, T. Kaisho, J. M. Norman, D. Mucida, M. Suematsu, T. Yaguchi, V. Bucci, T. Inoue, Y. Kawakami, B. Olle, B. Roberts, M. Hattori, R. J. Xavier, K. Atarashi, K. Honda, A defined commensal consortium elicits CD8 T cells and anti-cancer immunity. *Nature*. **565**, 600–605 (2019).
22. L. Gamboa, A. H. Zamat, D. Vanover, C. A. Thiveaud, H. E. Peck, H. Phuengkham, A. Sivakumar, A. M. Harris, S. N. Dahotre, F.-Y. Su, P. J. Santangelo, G. A. Kwong, Sensitizing solid tumors to CAR-mediated cytotoxicity using synthetic antigens (2021), p. 2021.12.11.472238, , doi:10.1101/2021.12.11.472238.
23. A. K. Erickson, P. R. Jesudhasan, M. J. Mayer, A. Narbad, S. E. Winter, J. K. Pfeiffer, Bacteria Facilitate Enteric Virus Co-infection of Mammalian Cells and Promote Genetic Recombination. *Cell Host Microbe*. **23**, 77-88.e5 (2018).
24. C. M. Robinson, P. R. Jesudhasan, J. K. Pfeiffer, Bacterial lipopolysaccharide binding enhances virion stability and promotes environmental fitness of an enteric virus. *Cell Host Microbe*. **15**, 36–46 (2014).
25. S. K. Kuss, G. T. Best, C. A. Etheredge, A. J. Pruijssers, J. M. Frierson, L. V. Hooper, T. S. Dermody, J. K. Pfeiffer, Intestinal microbiota promote enteric virus replication and systemic pathogenesis. *Science*. **334**, 249–252 (2011).
26. A. Haraga, M. B. Ohlson, S. I. Miller, Salmonellae interplay with host cells. *Nat Rev Microbiol*. **6**, 53–66 (2008).
27. X. Xu, W. A. H. Hegazy, L. Guo, X. Gao, A. N. Courtney, S. Kurbanov, D. Liu, G. Tian, E. R. Manuel, D. J. Diamond, M. Hensel, L. S. Metelitsa, Development of an Effective Cancer Vaccine Using Attenuated Salmonella and Type III Secretion System to Deliver Recombinant Tumor-Associated Antigens. *Cancer Res*. **74**, 6260–6270 (2014).
28. E. R. Manuel, C. A. Blache, R. Paquette, T. I. Kaltcheva, H. Ishizaki, J. D. I. Ellenhorn, M. Hensel, L. Metelitsa, D. J. Diamond, Enhancement of cancer vaccine therapy by systemic delivery of a tumor-targeting Salmonella-based STAT3 shRNA suppresses the growth of established melanoma tumors. *Cancer Res*. **71**, 4183–4191 (2011).
29. W. A. H. Hegazy, X. Xu, L. Metelitsa, M. Hensel, Evaluation of Salmonella enterica type III secretion system effector proteins as carriers for heterologous vaccine antigens. *Infect Immun*. **80**, 1193–1202 (2012).
30. X. Xu, M. I. Husseiny, A. Goldwich, M. Hensel, Efficacy of intracellular activated promoters for generation of Salmonella-based vaccines. *Infect Immun*. **78**, 4828–4838 (2010).

31. M. I. Husseiny, F. Wartha, M. Hensel, Recombinant vaccines based on translocated effector proteins of Salmonella Pathogenicity Island 2. *Vaccine*. **25**, 185–193 (2007).
32. A. K. Lee, C. S. Detweiler, S. Falkow, OmpR regulates the two-component system SsrA-ssrB in Salmonella pathogenicity island 2. *J Bacteriol*. **182**, 771–781 (2000).
33. A. Chabloz, J. V. Schaefer, I. Kozieradzki, S. J. F. Cronin, D. Strebinger, F. Macaluso, J. Wald, T. H. Rabbitts, A. Plückthun, T. C. Marlovits, J. M. Penninger, Salmonella-based platform for efficient delivery of functional binding proteins to the cytosol. *Commun Biol*. **3**, 342 (2020).
34. D. M. Widmaier, D. Tullman-Ercek, E. A. Mirsky, R. Hill, S. Govindarajan, J. Minshull, C. A. Voigt, Engineering the Salmonella type III secretion system to export spider silk monomers. *Mol Syst Biol*. **5**, 309 (2009).
35. S. L. Fink, B. T. Cookson, Pyroptosis and host cell death responses during Salmonella infection. *Cell Microbiol*. **9**, 2562–2570 (2007).
36. C. Schoen, A. Kolb-Mäurer, G. Geginat, D. Löffler, B. Bergmann, J. Stritzker, A. A. Szalay, S. Pilgrim, W. Goebel, Bacterial delivery of functional messenger RNA to mammalian cells. *Cell Microbiol*. **7**, 709–724 (2005).
37. X. Xu, M. Hensel, Systematic analysis of the SsrAB virulon of Salmonella enterica. *Infect Immun*. **78**, 49–58 (2010).
38. G. Xiong, M. I. Husseiny, L. Song, A. Erdreich-Epstein, G. M. Shackleford, R. C. Seeger, D. Jäckel, M. Hensel, L. S. Metelitsa, Novel cancer vaccine based on genes of Salmonella pathogenicity island 2. *Int J Cancer*. **126**, 2622–2634 (2010).
39. E. L. Hohmann, C. A. Oletta, S. I. Miller, Evaluation of a phoP/phoQ-deleted, aroA-deleted live oral Salmonella typhi vaccine strain in human volunteers. *Vaccine*. **14**, 19–24 (1996).
40. S. K. Doamekpor, S. Sharma, M. Kiledjian, L. Tong, Recent insights into noncanonical 5' capping and decapping of RNA. *J Biol Chem*. **298**, 102171 (2022).
41. R. Francisco-Velilla, A. Embarc-Buh, S. Abellan, E. Martinez-Salas, Picornavirus translation strategies. *FEBS Open Bio*. **12**, 1125–1141 (2022).
42. D. C. Ansardi, D. C. Porter, C. A. Jackson, G. Y. Gillespie, C. D. Morrow, RNA replicons derived from poliovirus are directly oncolytic for human tumor cells of diverse origins. *Cancer Res*. **61**, 8470–8479 (2001).
43. M. O. Din, T. Danino, A. Prindle, M. Skalak, J. Selimkhanov, K. Allen, E. Julio, E. Atolia, L. S. Tsimring, S. N. Bhatia, J. Hasty, Synchronized cycles of bacterial lysis for in vivo delivery. *Nature*. **536**, 81–85 (2016).
44. H. Loessner, A. Endmann, S. Leschner, K. Westphal, M. Rohde, T. Miloud, G. Hämmerling, K. Neuhaus, S. Weiss, Remote control of tumour-targeted Salmonella enterica serovar Typhimurium by the use of L-arabinose as inducer of bacterial gene expression in vivo. *Cell Microbiol*. **9**, 1529–1537 (2007).
45. A. K. Orta, N. Riera, Y. E. Li, S. Tanaka, H. G. Yun, L. Klaic, W. M. Clemons, The mechanism of the phage-encoded protein antibiotic from ΦX174. *Science*. **381**, eadg9091 (2023).
46. A. J. Wallace, T. J. Stillman, A. Atkins, S. J. Jamieson, P. A. Bullough, J. Green, P. J. Artymiuk, E. coli hemolysin E (HlyE, ClyA, SheA): X-ray crystal structure of the toxin and observation of membrane pores by electron microscopy. *Cell*. **100**, 265–276 (2000).
47. C. R. Beuzón, S. Méresse, K. E. Unsworth, J. Ruíz-Albert, S. Garvis, S. R. Waterman, T. A. Ryder, E. Boucrot, D. W. Holden, Salmonella maintains the integrity of its intracellular vacuole through the action of SifA. *EMBO J*. **19**, 3235–3249 (2000).
48. P. S. Reddy, K. D. Burroughs, L. M. Hales, S. Ganesh, B. H. Jones, N. Idamakanti, C. Hay, S. S. Li, K. L. Skele, A.-J. Vasko, J. Yang, D. N. Watkins, C. M. Rudin, P. L. Hallenbeck, Seneca Valley virus, a systemically deliverable oncolytic picornavirus, and the treatment of neuroendocrine cancers. *J Natl Cancer Inst*. **99**, 1623–1633 (2007).

49. M. J. Burke, Oncolytic Seneca Valley Virus: past perspectives and future directions. *Oncolytic Virother*. **5**, 81–89 (2016).
50. C. M. Rudin, J. T. Poirier, N. N. Senzer, J. Stephenson, D. Loesch, K. D. Burroughs, P. S. Reddy, C. L. Hann, P. L. Hallenbeck, Phase I clinical study of Seneca Valley Virus (SVV-001), a replication-competent picornavirus, in advanced solid tumors with neuroendocrine features. *Clin Cancer Res*. **17**, 888–895 (2011).
51. C. L. Morton, P. J. Houghton, E. A. Kolb, R. Gorlick, C. P. Reynolds, M. H. Kang, J. M. Maris, S. T. Keir, J. Wu, M. A. Smith, Initial testing of the replication competent Seneca Valley virus (NTX-010) by the pediatric preclinical testing program. *Pediatr Blood Cancer*. **55**, 295–303 (2010).
52. J. T. Poirier, P. S. Reddy, N. Idamakanti, S. S. Li, K. L. Stump, K. D. Burroughs, P. L. Hallenbeck, C. M. Rudin, Characterization of a full-length infectious cDNA clone and a GFP reporter derivative of the oncolytic picornavirus SVV-001. *J Gen Virol*. **93**, 2606–2613 (2012).
53. T. S. Miest, R. Cattaneo, New viruses for cancer therapy: meeting clinical needs. *Nat Rev Microbiol*. **12**, 23–34 (2014).
54. A. C. Palmenberg, Proteolytic processing of picornaviral polyprotein. *Annu Rev Microbiol*. **44**, 603–623 (1990).
55. R. B. Kapust, J. Tözsér, T. D. Copeland, D. S. Waugh, The P1' specificity of tobacco etch virus protease. *Biochem Biophys Res Commun*. **294**, 949–955 (2002).
56. L. D. Cabrita, D. Gilis, A. L. Robertson, Y. Dehouck, M. Rooman, S. P. Bottomley, Enhancing the stability and solubility of TEV protease using in silico design. *Protein Science*. **16**, 2360–2367 (2007).
57. S. van den Berg, P.-A. Löfdahl, T. Härd, H. Berglund, Improved solubility of TEV protease by directed evolution. *J Biotechnol*. **121**, 291–298 (2006).
58. M. Aguilar Rangel, P. T. Dolan, S. Taguwa, Y. Xiao, R. Andino, J. Frydman, High-resolution mapping reveals the mechanism and contribution of genome insertions and deletions to RNA virus evolution. *Proc Natl Acad Sci U S A*. **120**, e2304667120 (2023).
59. W. G. Dougherty, S. M. Cary, T. D. Parks, Molecular genetic analysis of a plant virus polyprotein cleavage site: a model. *Virology*. **171**, 356–364 (1989).
60. Z. Zhang, L. Hua, A. Gupta, D. Tricoli, K. J. Edwards, B. Yang, W. Li, Development of an Agrobacterium-delivered CRISPR/Cas9 system for wheat genome editing. *Plant Biotechnol J*. **17**, 1623–1635 (2019).
61. W. Schaffner, Direct transfer of cloned genes from bacteria to mammalian cells. *Proceedings of the National Academy of Sciences*. **77**, 2163–2167 (1980).
62. K. Narayanan, P. E. Warburton, DNA modification and functional delivery into human cells using Escherichia coli DH10B. *Nucleic Acids Res*. **31**, e51 (2003).
63. C. Grillot-Courvalin, S. Goussard, F. Huetz, D. M. Ojcius, P. Courvalin, Functional gene transfer from intracellular bacteria to mammalian cells. *Nat Biotechnol*. **16**, 862–866 (1998).
64. C. Grillot-Courvalin, S. Goussard, P. Courvalin, Wild-type intracellular bacteria deliver DNA into mammalian cells. *Cell Microbiol*. **4**, 177–186 (2002).
65. W. Kong, S.-Y. Wanda, X. Zhang, W. Bollen, S. A. Tinge, K. L. Roland, R. Curtiss, Regulated programmed lysis of recombinant Salmonella in host tissues to release protective antigens and confer biological containment. *Proc Natl Acad Sci U S A*. **105**, 9361–9366 (2008).
66. W. Kong, M. Brovold, B. A. Koeneman, J. Clark-Curtiss, R. Curtiss, Turning self-destructing Salmonella into a universal DNA vaccine delivery platform. *Proc Natl Acad Sci U S A*. **109**, 19414–19419 (2012).
67. S. Xiang, J. Fruehauf, C. J. Li, Short hairpin RNA-expressing bacteria elicit RNA interference in mammals. *Nat Biotechnol*. **24**, 697–702 (2006).

68. H. Guo, J. Zhang, C. Inal, T. Nguyen, J. H. Fruehauf, A. C. Keates, C. J. Li, Targeting tumor gene by shRNA-expressing Salmonella-mediated RNAi. *Gene Ther*. **18**, 95–105 (2011).
69. S. Weiss, T. Chakraborty, Transfer of eukaryotic expression plasmids to mammalian host cells by bacterial carriers. *Curr Opin Biotechnol*. **12**, 467–472 (2001).
70. A. Acevedo, L. Brodsky, R. Andino, Mutational and fitness landscapes of an RNA virus revealed through population sequencing. *Nature*. **505**, 686–690 (2014).
71. J. W. Drake, Rates of spontaneous mutation among RNA viruses. *Proc Natl Acad Sci U S A*. **90**, 4171–4175 (1993).
72. R. Sanjuán, M. R. Nebot, N. Chirico, L. M. Mansky, R. Belshaw, Viral mutation rates. *J Virol*. **84**, 9733–9748 (2010).
73. E. Domingo, C. García-Crespo, R. Lobo-Vega, C. Perales, Mutation Rates, Mutation Frequencies, and Proofreading-Repair Activities in RNA Virus Genetics. *Viruses*. **13**, 1882 (2021).
74. K. A. Datsenko, B. L. Wanner, One-step inactivation of chromosomal genes in Escherichia coli K-12 using PCR products. *Proc Natl Acad Sci U S A*. **97**, 6640–6645 (2000).
75. Z. S. Singer, P. M. Ambrose, T. Danino, C. M. Rice, Quantitative measurements of early alphaviral replication dynamics in single cells reveals the basis for superinfection exclusion. *Cell Syst*. **12**, 210-219.e3 (2021).